Probing the Role of the Fe−S Subunit Hinge Region during Q_o Site Catalysis in *Rhodobacter capsulatus* bc_1 Complex[†]

Elisabeth Darrouzet, Maria Valkova-Valchanova, and Fevzi Daldal*

Department of Biology, Plant Science Institute, University of Pennsylvania, Philadelphia, Pennsylvania 19104

Received April 3, 2000; Revised Manuscript Received August 14, 2000

ABSTRACT: The ubihydroquinone:cytochrome *c* oxidoreductase, or bc_1 complex, functions according to a mechanism known as the modified Q cycle. Recent crystallographic data have revealed that the extrinsic domain containing the [2Fe2S] cluster of the Fe−S subunit of this enzyme occupies different positions in various crystal forms, suggesting that this subunit may move during ubihydroquinone oxidation. As in these structures the hydrophobic membrane anchor of the Fe−S subunit remains at the same position, the movement of the [2Fe2S] cluster domain would require conformational changes of the hinge region linking its membrane anchor to its extrinsic domain. To probe the role of the hinge region, *Rhodobacter capsulatus* bc_1 complex was used as a model, and various mutations altering the hinge region amino acid sequence, length, and flexibility were obtained. The effects of these modifications on the bc_1 complex function and assembly were investigated in detail. These studies demonstrated that the nature of the amino acid residues located in the hinge region (positions 43−49) of *R. capsulatus* Fe−S subunit was not essential per se for the function of the bc_1 complex. Mutants with a shorter hinge (up to five amino acid residues deletion) yielded functional bc_1 complexes, but contained substoichiometric amounts of the Fe−S subunit. Moreover, mutants with increased rigidity or flexibility of the hinge region altered both the function and the assembly or the steady-state stability of the bc_1 complex. In particular, the extrinsic domain of the Fe−S subunit of a mutant containing six proline residues in the hinge region was shown to be locked in a position similar to that seen in the presence of stigmatellin. Interestingly, the latter mutant readily overcomes this functional defect by accumulating an additional mutation which shortens the length of the hinge. These findings indicate that the hinge region of the Fe−S subunit of bacterial bc_1 complexes has a remarkable structural plasticity.

The ubihydroquinone:cytochrome *c* oxidoreductase, or the bc_1[1] complex, is a key component of mitochondrial and bacterial respiratory chains and also of the cyclic photosynthesis in bacteria (for review see refs *1*−*4*). Moreover, a homologous complex (the b_6f complex) also plays a similar role in photosynthetic electron transfer in cyanobacteria, algae, and higher plant chloroplasts (for a review, see ref *5*). This integral membrane protein conveys electrons from hydroquinone derivatives to *c*-type cytochromes (cyt *c* in mitochondria, cyt c_2 or cyt c_y in *Rhodobacter capsulatus*) or plastocyanine, along with the translocation of protons across the membrane, setting up a proton gradient subsequently used for ATP synthesis.

In prokaryotic organisms, the bc_1 complex is usually composed of three subunits, encoded by genes organized as an operon called *pet*ABC or *fbc*FBC (for reviews see refs *1*, *2*, and *4*), and bearing one *c*-type heme (cyt c_1), two *b*-type hemes (cyt *b*) and one [2Fe2S] metal cluster (Fe−S subunit). The mechanism of function of the bc_1 complex relies on the existence of two catalytic sites (Q_i and Q_o) located on each side of the membrane. During the oxidation of a QH_2 at the Q_o site, one of the two electrons is transferred to the high potential redox chain of the bc_1 complex via first the reduction of the [2Fe2S] cluster of the Fe−S subunit, and then the heme of cyt c_1. The other electron is conveyed to the low potential chain, constituted of the hemes b_L and b_H (*6*−*8*), and then to the ubiquinone at the Q_i site. The key to the energetic efficiency of the bc_1 complex (i.e., translocation of two protons per one electron) relies on this bifurcation of electrons, but the precise mechanism governing this event remains unknown. During the last three years, an intriguing hypothesis has emerged from the resolution of several three-dimensional structures of the bc_1 complex. Indeed, in the first crystal structure of the mitochondrial bc_1 complex obtained by Xia et al. (*9*), the distance (31 Å) calculated between the [2Fe2S] cluster of the Fe−S subunit and heme c_1 was far too large to support the fast electron-transfer rate observed between these two cofactors. Later on, several structures for mitochondrial bc_1 complexes in the presence or absence of various inhibitors have revealed different positions of the [2Fe2S] cluster domain within the enzyme

[†] This work was supported by NIH Grant GM 38237 to F.D.

* To whom correspondence should be addressed. Phone: (215) 898-4394. Fax: (215) 898-8780. E-mail: fdaldal@sas.upenn.edu.

[1] Abbreviations: cyt, cytochrome; bc_1 complex, ubihydroquinone-cytochrome *c* oxidoreductase; b_H, high potential *b*-type heme; b_L, low potential *b*-type heme; b_6f complex, plastohydroquinone plastocyanine oxidoreductase; DAD, 2,3,5,6-tetramethyl-1,4-phenylenediamine; DBH_2, 2,3-dimethoxy-5-methyl-6-decyl-1,4-benzohydroquinone; DDM, dodecyl maltoside; EDTA, ethylenediaminetetraacetic acid; E_h, ambient potential; E_{m7}, redox midpoint potential at pH 7; EPR, electron paramagnetic resonance; MOPS, 3-(*N*-morpholino)propanesulfonic acid; PES, *N*-ethyl-dibenzopyrazine ethyl sulfate; PMS, *N*-methyl-dibenzopyrazine methyl sulfate; PMSF, phenylmethanesulfonyl fluoride; Ps, photosynthesis; Q_o, ubihydroquinone oxidation site; Q_i, ubiquinone reduction site; RC, reaction center; SDS, sodium dodecyl sulfate; SDS−PAGE, sodium dodecyl sulfate−polyacrylamide gel electrophoresis; SHE, standard hydrogen electrode; Tris, tris(hydroxymethyl)aminomethane; [2Fe2S], two iron−two sulfur cluster.

10.1021/bi000750l CCC: $19.00
Published on Web 11/22/2000

complex (*10*−*12*). Yet, none of these positions fits completely with the entire catalytic mechanism. The cleft observed between the Fe−S subunit and cyt *b* when the [2Fe2S] cluster domain is located closer to cyt c_1 is hardly compatible with the fact that the occupants of the Q_o site (Q/QH_2 and inhibitors) interact with both the Fe−S subunit and cyt *b*. Thus, the idea that the Fe−S subunit may move during catalysis was originated (*10*) as part of a mechanism allowing bifurcation of electrons at the Q_o site. However, it remains unknown whether the different locations of the Fe−S subunit observed in various crystals reflect the various conformations of this subunit during the catalytic cycle of the bc_1 complex or are mediated by the crystal contacts or the presence of inhibitors. A comparison of various structures indicates that the membrane anchor domain of the Fe−S subunit stays fixed, and the structure of the [2Fe2S] cluster domain does not change appreciably. Thus, the movement of the cluster domain of the Fe−S subunit would require conformational changes of the hinge region that connects these two domains. Recently, Tian et al. (*13*, *14*) have shown that in *Rhodobacter sphaeroides*, increasing the rigidity of the Fe−S subunit hinge by incorporation of either several proline residues or two cysteine residues, which are able to form a disulfide bond, alters the function of the bc_1 complex. We have also demonstrated that in *R. capsulatus* extending the length of the hinge region abolishes the activity of the bc_1 complex (*15*). In addition, mutations affecting the corresponding region of the Fe−S subunit of yeast mitochondria (*16*) or of *Chlamydomonas* chloroplast (*17*) have also been reported.

In this work, extensive mutagenesis of the Fe−S subunit hinge region was undertaken using *R. capsulatus* bc_1 complex. The studies indicated that a shorter hinge (up to a deletion of five amino acid residues) yields functional bc_1 complexes, but with a substoichiometry of the Fe−S subunit in respect to the other subunits. Importantly, an excessive rigidity or flexibility of the hinge affects drastically the activity of this enzyme, but this can be overcome by shortening the length of the hinge domain. Therefore, the hinge region of the Fe−S subunit requires an optimal combination of flexibility and length without a need for a specific amino acid side chain at any given position, to confer both steady-state stability and catalytic activity to the bc_1 complex, including the movement of its Fe−S subunit.

MATERIALS AND METHODS

Bacterial Strains and Growth. Escherichia coli and *R. capsulatus* strains were grown as described in ref *18* in the presence of appropriate antibiotics. Photosynthetic growth (Ps) of *R. capsulatus* strains was at 35 °C under continuous light and anaerobic conditions, and respiratory growth at the same temperature in the dark under semiaerobic conditions. MT-RBC1 is a bc_1^- strain where the chromosomal copy of the *petABC* operon has been deleted and replaced by a gene cartridge conferring resistance to spectinomycin (*18*). The strain pMTS1/MT-RBC1 corresponds to MT-RBC1 complemented in trans with the plasmid pMTS1, which contains a kanamycin resistance cartridge and a wild-type copy of *petABC*.

Genetic Techniques. A silent unique site (*Mlu*I) changing the codon corresponding to Ala40 of the Fe−S subunit from GCT to GCG was introduced by using the QuickChange site-directed mutagenesis Kit (Stratagene). For this purpose, plasmid pPET1 (pBR322-derivative) bearing a wild-type copy of *petABC* (*18*) was used as a template with the primers Mlu1F and Mlu1R (Table 1). The DNA fragment bearing the mutation thus generated was cut with *Bst*XI and *Apa*LI and exchanged with its counterpart in pMTS1, yielding the plasmid pMTS1-Mlu1, which was used as the parental plasmid in this study. The various hinge mutants were engineered by PCR using a common upstream primer (5′-GTCTTGGGCTCGTAA-3′) corresponding to a location 5′ to *Apa*LI site and the appropriate downstream primers containing the silent *Mlu*I site and the desired mutation as listed in Table 1. The PCR fragments were cut with *Mlu*I and *Apa*LI restriction enzymes and exchanged with the wild-type counterpart in pMTS1-Mlu1. For each mutant, the presence of only the desired mutation on the insert thus exchanged was confirmed by subsequent DNA sequencing. All plasmids thus constructed were introduced into MT-RBC1 via triparental crosses as described previously (*18*).

Biochemical and Biophysical Techniques. Chromatophore membranes were prepared in MOPS buffer (50 mM, pH 7.0) containing 100 mM KCl, 1 mM EDTA and 1 mM PMSF, using a French pressure cell at 18 000 psi, as described in ref *18*. They were washed three times in the same buffer, and protein concentrations were determined according to ref *19*. Sodium dodecyl sulfate−polyacrylamide gel electrophoresis (SDS−PAGE) was performed using an acrylamide concentration of 15%, and gels were stained with Coomassie blue for proteins. Immunoblot analyses were performed with monoclonal antibodies specific for the subunits of *R. capsulatus* bc_1 complex. To estimate the stoichiometry of the Fe−S subunit in the bc_1 complex, SDS gels and immunoblots were scanned for densitometry analyses. The intensity ratio of the Fe−S subunit per cyt *b* or cyt c_1 subunits was then calculated, and compared to that obtained with the wild-type strain on the very same gel or immunoblot.

Thermolysin-mediated proteolysis of the Fe−S subunit using chromatophore membranes was performed at room temperature in 50 mM Tris-HCl, pH 8.0, containing 100 mM NaCl, 0.01% dodecyl maltoside (DDM), as described in Valkova-Valchanova et al. (*20*). Briefly, chromatophore membranes containing 500−850 μg of proteins were digested for 1 h with 0.02 nmol of thermolysin in the presence or absence of 2 mM stigmatellin. In these experiments, a large excess of inhibitor was used, for it was observed that stigmatellin purchased from Fluka loses its activity very rapidly under our assay conditions. Aliquots were then analyzed by immunoblotting using polyclonal antibodies against the Fe−S subunit of *R. capsulatus*, and the amount of the 18 kDa fragment thus generated was determined.

DBH_2:cyt *c* reductase assays were performed as described earlier in ref *18*. Optical difference spectra for *b*- and *c*-type cytochromes were recorded as in ref *21*. Flash-induced, single-turnover kinetics for cyt *c* or cyt *b* reduction were performed as described in ref *22* using chromatophore membranes and a single wavelength spectrophotometer (Biomedical Instrumentation Group, University of Pennsylvania, Philadelphia, PA) in the presence of 2.5 μM valinomycin, PMS, PES, DAD, and 2-hydroxy-1,4-naphthoquinone. The quantity of chromatophore membranes used in the assays corresponded to 0.2−0.35 μM reaction center, whose

Table 1: Plasmids and Nucleotide Primers Used in This Study

Plasmid	[a]Amino acid sequence modified	[a]Nucleotide sequence of the primers used
pMTS1	$_{40}$ASADVKAMASIFV$_{52}$	[b]C CAA ATG AAC GCT TCG GCC GAC GTC AAG GCG
pMTS1-Mlu1	ASADVKAMASIFV	Mlu1F:C CAA ATG AAC GCG TCG GCC GAC GTC AAG GCG
		Mlu1R:GAC GTC GGC CGA CGC GTT CAT TTG GTT GAT CAA CGG
pR:D43X	ASAXVKAMASIFV	ATG AAC GCG TCG GCC XXX GTC AAG GCG ATG GC
X=E, G, H, N, S		with XXX= GRG, CDC or ARC
pR:V44A	ASADAKAMASIFV	ATG AAC GCG TCG GCC GAC GCC AAG GCG ATG GC
pR:K45A	ASADVAAMASIFV	ATG AAC GCG TCG GCC GAC GTC GCG GCG ATG GCA TCG
pR:M47A	ASADVKAAASIFV	ATG AAC GCG TCG GCC GAC GTC AAG GCG GCG GCA TCG ATC TTC G
pR:S49A	ASADVKAMAAIFV	ATG AAC GCG TCG GCC GAC GTC AAG GCG ATG GCA GCG ATC TTC G
Δ1	ASADVK-MASIFV	ATG AAC GCG TCG GCC GAC GTC AAG ATG GCA TCG ATC TTC G
Δ3	ASADV---ASIFV	ATG AAC GCG TCG GCC GAC GTC GCA TCG ATC TTC GTC G
Δ5	ASAD-----SIFV	ATG AAC GCG TCG GCC GAC TCG ATC TTC GTC G
Δ7	ASA-------IFV	ATG AAC GCG TCG GCC ATC TTC GTC GAT G
6Pro	ASADPPPPPPIFV	ATG AAC GCG TCG GCC GAC CCG CCG CCG CCG CCG CCG ATC TTC GTC GAT G
6Gly	ASADGGGGGGIFV	ATG AAC GCG TCG GCC GAC GGC GGC GGC GGC GGC GGC ATC TTC GTC GAT G
+3AlaΔ3	ASADVKAAAAIFV	[b]ATG AAC GCG TCG GCC GAC GTC AAG GCG GCG GCG GCG ATC TTC G
3ProΔ3	ASAD-PPP—IFV	[b]ATG AAC GCG TCG GCC GAC CCG CCG CCG ATC TTC GTC GAT G
3GlyΔ3	ASAD-GGG—IFV	[b]ATG AAC GCG TCG GCC GAC GGC GGC GGC ATC TTC GTC GAT G

[a] The amino acid sequences shown correspond to residues 40−52 encompassing the hinge region of the Fe−S subunit; the nucleotide sequences of the primers used to generate various mutations are given in the 5′-3′ orientation. [b] For pMTS1, +3AlaΔ3, 3ProΔ3, 3GlyΔ3, the nucleotide sequences shown are the DNA sequences of the region.

concentration was determined by measuring the optical absorbance difference between 605 and 540 nm at an E_h of 380 mV, using an extinction coefficient of 29.8 mM^{-1} cm^{-1}. Transient cyt *c* and cyt *b* reduction kinetics initiated by a short saturating flash (8 μs) from a xenon lamp were followed at 550−540 nm and 560−570 nm, respectively. The concentration of antimycin A, myxothiazol, and stigmatellin used were 5, 5, and 1 μM, respectively, and the E_h was poised at 100 mV. EPR spectroscopy was performed using a Bruker ESP-300E, equipped with an Oxford Instruments ESR-9 helium cryostat, and EPR recording conditions were as follows: sample temperature, 20 K; microwave power, 2 mW; modulation amplitude, 20.243 G; modulation frequency, 100 kHz; microwave frequency, 9.45 GHz. For these experiments, the concentration of chromatophore membranes was 25−30 mg of protein/mL, and the samples with Q pool oxidized were obtained by incubating them on ice for 10 min with 20 mM ascorbate, in the presence or absence of 100 μM stigmatellin. Oxidative titrations of the Fe−S subunit [2Fe2S] cluster in chromatophore membranes were conducted potentiometrically according to Dutton (*23*), in the presence of 100 μM tetrachlorohydroquinone, DAD, 1,2-naphthoquinone-4-sulfonate, and 1,2-naphthoquinone.

Chemicals. All chemicals were as described earlier (*24*).

RESULTS

The Nature of the Amino Acid Residues Located between the Positions 43 and 49 of the Fe−S Subunit Is Not Essential for the Function of the bc_1 Complex. Amino acid sequence alignment of the hinge region of the Fe−S subunit reveals a high degree of identity between bacteria, yeast, mammals, fungi, and even with the corresponding region of the plant bc_1 complex (Figure 1). Thus, to probe whether any of these amino acid residues is required for the function of the bc_1 complex, the region between the positions 43 and 49 of the Fe−S subunit was first scanned using single alanine mutations. In addition, the highly conserved residue D43 (D67 in bovine sequence) which is located in the dimeric structure of the bovine enzyme in close vicinity to both cyt *b* monomers and to one of the cyt c_1 subunits was replaced by various residues (Figure 1). All of these mutations yielded

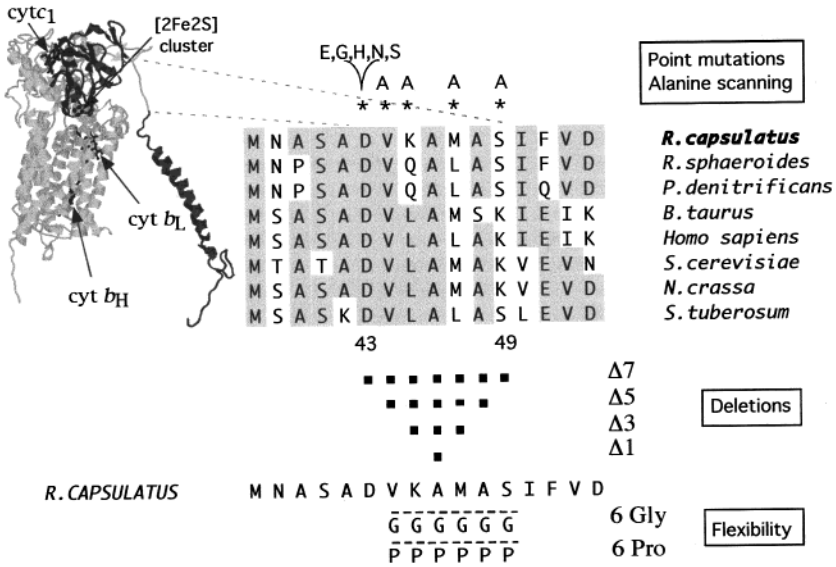

FIGURE 1: Various *R. capsulatus* Fe−S subunit hinge region mutations. The structure of the three catalytic subunits of the chicken heart cyt bc_1 in the presence of stigmatellin (*10*) is represented on the left side of the panel, with the Fe−S subunit in dark gray. On the right side, the Fe−S subunit sequences from a few selected species aligned with that of *R. capsulatus* between the positions 38 and 53 (*R. capsulatus* numbering) and the positions of the different mutations are shown. Identical residues are highlighted in gray. Asterisks (*) and squares (■) refer to the point mutations and deletions, respectively, and the single amino acid substitutions are shown above the sequences. The six proline or six glycine residues in the mutants "6Pro" or "6Gly" replace the six natural amino acid residues of the native protein between the positions 44 and 49.

Table 2: Characteristics of the Fe−S Subunit Hinge Mutants

strains	Ps phenotype (dt in min)[a]	bc_1 complex activity (%)[b]	electron-transfer rate (%)[c]	assembly (%) Fe−S subunit[d]	assembly (%) [2Fe-2S] cluster[e]
wild-type	Ps^+ (110)	100	100	100	100
D43E, G, H, N, S	Ps^+ (nd)	40−70	90−100	45−85	50−75
V44A, K45A, M47A, S49A	Ps^+ (nd)	80−110	65−125	≥100	75−100
Δ1	Ps^+ (120)	30	45	65	65
Δ3	Ps^+ (125)	3	45	30	35
Δ5	Ps^+ (130)	0	7	20	5
Δ7[f]	Ps^- (na)	0	0	30	15
6Pro[f]	Ps^- (na)	0	1	50	60
6Gly[f]	$Ps^{+/-}$ (210)[a]	3	10	60	60
+3AlaΔ3[g]	Ps^+ (nd)	100	nd	nd	nd
3ProΔ3[g]	Ps slow (150)	0	15	nd	nd
3GlyΔ3[g]	Ps^+ (135)	0	12	nd	nd

[a] Ps^+ or Ps^- indicates ability or inability, respectively, to grow photosynthetically in MPYE enriched medium, and dt is the doubling time in minutes. The doubling time for the 6Gly mutant is probably influenced by the likely appearance of revertants in the culture. [b] Steady-state bc_1 complex activity was determined by measuring the DBH_2: cyt *c* reductase activity expressed as percentage of the wild-type activity, which was in this instance 3.4 μmol of cyt *c* reduced per min per mg of membrane proteins. [c] Electron-transfer rate reflects single turnover bc_1 complex activity and corresponds to the average of QH_2 to cyt *c* and QH_2 to cyt *b* electron transfer rates. These rates expressed as a percentage of that of the wild type enzyme were not significantly different from each other. They were determined by recording cyt *c* rereduction kinetics at 550−540 nm, and cyt *b* reduction at 560−570 nm in the presence of 5 μM antimycin, at an ambient potential E_h of 100 mV. The traces were fitted to a single exponential equation, and the results expressed as a percentage of the wild-type activities, which were approximately 300 and 500 s^{-1} for cyt *c* rereduction kinetics and cyt *b* reduction, respectively. [d] Assembly Fe−S subunit refers to the stoichiometry of the Fe−S subunit to cyt c_1 or cyt *b* subunits as determined by scanning of the SDS−PAGE gels and immunoblots as described in Materials and Methods, and expressed as a percentage of the wild-type. [e] Assembly [2Fe-2S] cluster refers to the relative amounts of the [2Fe-2S] cluster in the mutants in comparison to the wild-type, as determined by the amplitude of their EPR g_y signal normalized for protein concentrations of chromatophore membranes. [f] The frequency of reversion to Ps^+ phenotype of the Δ7, 6Pro and 6Gly strains were $<10^{-9}$, 10^{-6}, and $>10^{-4}$, respectively. [g] +3AlaΔ3, 3ProΔ3, and 3GlyΔ3 mutants correspond to a mutant with an insertion of three alanine residues at position 46 followed by a deletion of the residues initially numbered 47, 48, and 49, a mutant containing six proline residues from positions 44 to 49 of which three have been deleted subsequently, and a mutant containing six glycine residues from positions 44 to 49 of which three have been deleted subsequently, respectively. nd, not done; na, nonavailable.

mutants that grew photosynthetically (Ps^+) and contained highly active bc_1 complexes, with quasinormal steady-state and single turnover activities (Table 2). Therefore, none of the amino acid residues located between the positions 43 and 49 was essential for the function of *R. capsulatus* bc_1 complex.

Fe−S Subunit Mutants with a Shorter Hinge Region. Further insight into the structure and function of the hinge region of the Fe−S subunit was obtained by the analysis of mutations shortening it by one, three, five, and seven amino acid residues centered around position 46 (Δ1, Δ3, Δ5, and Δ7 mutants, respectively) (Figure 1). Surprisingly, of these deletions only the Δ7 mutation that removed the entire hinge region from position 43 and 49 was unable to support Ps growth of *R. capsulatus*. The Δ1 mutant which eliminated position 46, Δ3 which eliminated positions 45−46−47, and Δ5 which eliminated positions 44−45−46−47−48 were all Ps^+ (doubling times of 120−130 min on MPYE medium

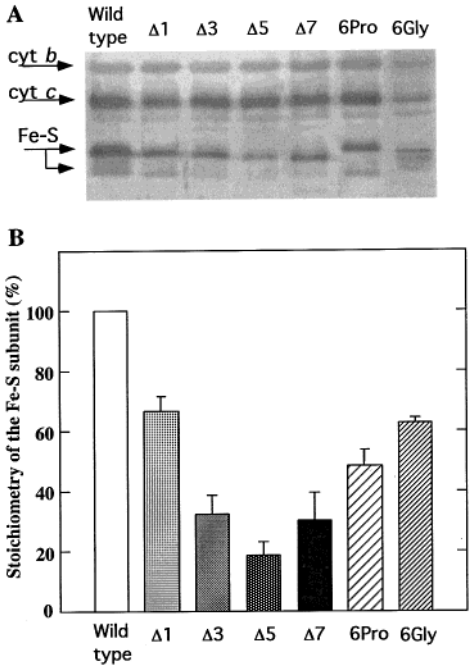

FIGURE 2: Steady-state assembly of the bc_1 complex in various Fe−S subunit hinge region mutants. A 15% SDS−polyacrylamide gel was blotted onto a PVDF membrane, and immunoprobed using monoclonal antibodies against the cyt *b*, cyt c_1, and the Fe−S subunits in chromatophore membranes (panel A). The bar diagram (panel B) represents the average stoichiometry of the Fe−S subunit in the bc_1 complex, estimated after scanning of several SDS−polyacryamide gels and immunoblots similar to that shown in panel A. For each mutant, the ratio of the Fe−S subunit to cyt *b* (or cyt c_1) subunit was determined, and normalized to the equivalent ratio obtained on the same gel or same immunoblot for the wild-type enzyme, and the standard deviations are also indicated. In all cases, lane 1 or bar 1 represents the wild-type, lanes 2, 3, 4, and 5 correspond to the Δ1, Δ3, Δ5, and Δ7 deletion mutants, respectively, and lanes 6 and 7 to the 6Pro and 6Gly mutants, respectively. Note the large effect on the Fe−S subunit migration of just a few amino acids deletion or the 6Pro or 6Gly substitutions.

versus 110 min for a wild-type strain) (Table 2). Detailed characterization of these mutants revealed that their bc_1 complex single-turnover activities were partially, and their steady-state activities were drastically, affected (Table 2).

To investigate whether in the deletion mutants the decrease or absence of bc_1 complex steady-state activity was due to a perturbed assembly or stability of the enzyme complex, the amounts of its subunits and cofactors were analyzed. The levels of the three subunits were determined by SDS−PAGE and immunoblot analyses (Figure 2, Table 2). The amounts of the *b*- and *c*-type hemes in the chromatophore membranes were measured spectroscopically via ascorbate or dithionite reduced *minus* ferricyanide oxidized optical difference spectra (data not shown), and by estimating the amounts of the [2Fe-2S] cluster by EPR spectroscopy (Figure 3, Table 2). The data indicated that in chromatophore membranes of the mutants the amounts of the *b*- and *c*-type hemes and cyt *b* and cyt *c* subunits per amount of total proteins were comparable to those found in a wild-type strain. On the other hand, the amount of the Fe−S subunit was decreased to varying degrees in all mutants (Figure 2, panels A and B). Especially in the Δ5 mutant, the amounts of the protein and the [2Fe2S] cluster were less than 20% of that found in a wild-type strain (Table 2). Moreover, preparations using intact cells, instead of chromatophore membranes, further confirmed the substoichiometric amounts of the Fe−S subunits in the mutants (not shown). Thus, the data established that shortening the length of the hinge region of the Fe−S subunit affected the stoichiometry of this subunit in the bc_1 complex without abolishing completely the enzymatic activity.

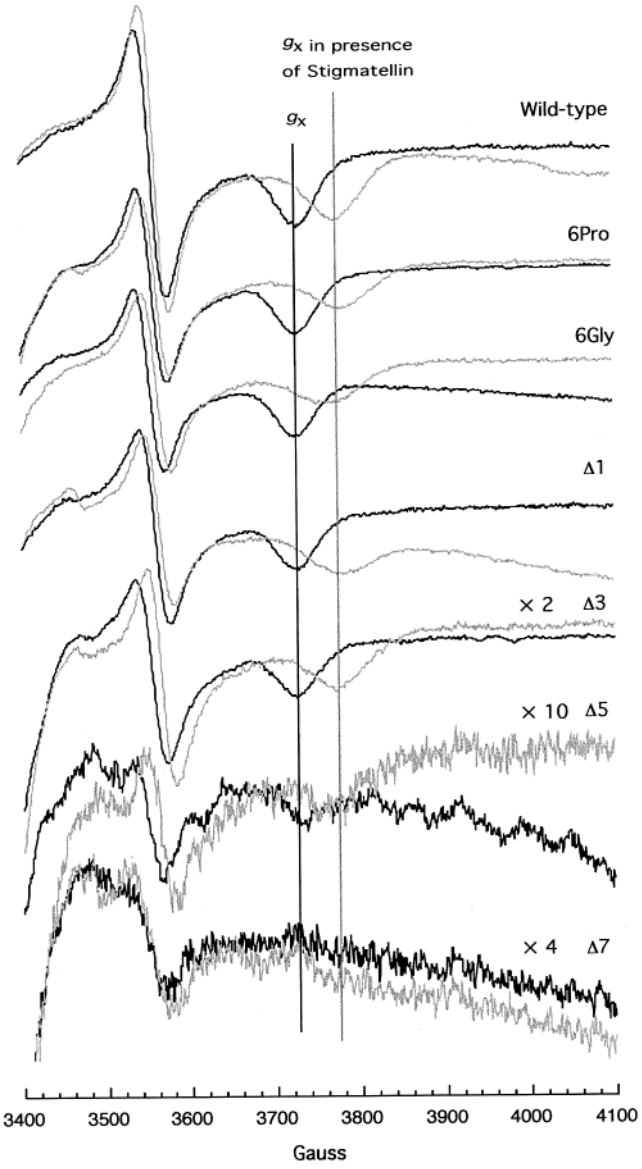

FIGURE 3: EPR spectra of the [2Fe2S] cluster in the presence or absence of stigmatellin in various Fe−S subunit hinge mutants. The EPR spectra of the wild-type and the different mutants were obtained using chromatophore membranes after ascorbate reduction of the cluster and with the EPR spectroscopy conditions described in the Materials and Methods. The darker and lighter traces represent the spectra obtained without inhibitor and in the presence of stigmatellin, respectively. Vertical lines indicate the wild-type g_x values, which are to be compared with those observed with the mutant strains. ×2, ×10, and ×4 indicate the scaling factor used to plot the spectra for the Δ3, Δ5, and Δ7 mutants, respectively, compared to the scale used for the wild-type strain and the 6Pro, 6Gly and Δ1 mutants.

Next, the integrity of the Q_o site in the mutants with a shorter hinge region was probed by using EPR spectroscopy. For all deletion mutants, with the exception of Δ7 mutant, the shape of the EPR spectra with Q pool oxidized in the presence or absence of stigmatellin was identical to that seen with a wild-type strain (Figure 3). In agreement with the substoichiometric amounts of the Fe−S subunits, the am-

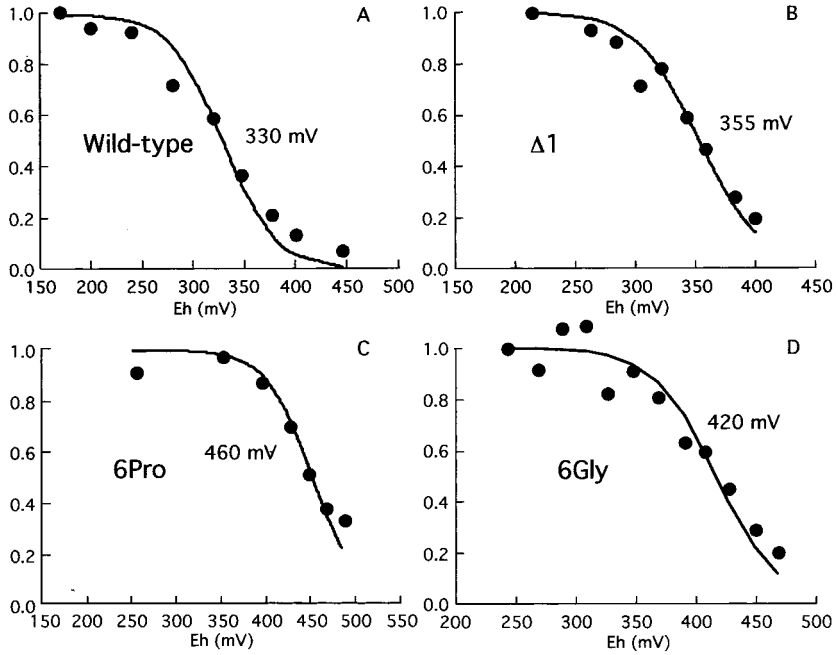

FIGURE 4: Potentiometric dark titrations of the [2Fe2S] cluster of the Fe−S subunit in various hinge mutants. The E_{m7} values of the [2Fe2S] cluster of the Fe−S subunit of the wild-type (panel A), Δ1 (panel B), 6Pro (panel C), and 6Gly (panel D) mutants were determined by recording the amplitude of the EPR g_y signal between 100 and 500 mV, as described in the Materials and Methods. In each case, the amplitudes observed at given E_h values were normalized and fitted to a $n = 1$ Nernst equation to deduce the indicated E_{m7} values.

plitudes of the g_y and g_x EPR signals per amount of total proteins were much smaller in the mutants (Figure 3, Table 2). In the case of the Δ7 mutant, no readily detectable interaction with the Q_o site residents Q/QH_2 or the inhibitor stigmatellin could be seen by EPR spectroscopy, indicating a major perturbation of the Q_o site in addition to the substoichiometry of the Fe−S subunit. The effects of the Δ1 or Δ3 mutations on the properties of the [2Fe2S] cluster of the Fe−S subunit were further investigated by determination of their E_{m7} values. While the E_{m7} value for the [2Fe2S] cluster is around 300−320 mV in chromatophore membranes of *R. capsulatus* (*25*), this value was increased to approximately 355 mV in the deletion mutants Δ1 and Δ3 (Figure 4, panel B, and not shown). Thus, a change in the structure of the hinge region must have modified the environment of the [2Fe2S] cluster at the Q_o pocket and increased its E_{m7} value. Due to the low amounts of the Fe−S subunits present in the Δ5 and Δ7 mutants, their E_{m7} values were not determined.

Fe−S Subunit Mutants Changing the Flexibility of the Hinge Region. Given that an appropriate length of the hinge region of the Fe−S subunit is important for its proper assembly to the bc_1 complex, we then attempted to modify its structural properties. Different mutants were engineered to change the flexibility of the hinge region by replacing its six amino acid residues located between the positions 44 and 49 with six glycine or six proline residues (Figure 1). Of the strains thus obtained, the 6Pro mutant was Ps^- while the 6Gly mutant grew poorly under Ps growth conditions. In addition, both mutants reverted with unusually high frequencies on MPYE enriched media (10^{-6} and $>10^{-4}$, respectively) (Table 2). In both mutants the Fe−S subunit was substoichiometric in comparison with a wild-type bc_1 complex as revealed by SDS−PAGE and immunoblot analyses (Figure 2). Nevertheless, they contained bc_1 complexes in amounts higher than what was present in some other Ps^+ mutants, like for example the Δ5 mutant. Considering that such amounts of assembled bc_1 complexes would have been otherwise sufficient to support Ps growth, the interactions between the [2Fe2S] cluster and the Q_o site residents were probed by EPR spectroscopy. No major differences in the EPR spectra of the 6Pro and 6Gly mutants were observed either with the Q_{pool} oxidized, or in the presence of stigmatellin, in comparison to wild-type spectra (Figure 3). However, determination of the E_m values of the [2Fe2S] cluster in the 6Pro and 6Gly mutants revealed that they were as high as 460 and 420 mV, respectively (Figure 4, panels C and D). These values are similar to the E_m value seen with a wild-type bc_1 complex inhibited with stigmatellin.

The Fe−S Subunit of the 6Pro Mutant Is Locked in the Q_o Pocket in a Location Similar to That Seen in the Presence of Stigmatellin. The high E_m value for the [2Fe2S] cluster of the Fe−S subunit of the 6Pro mutant led us to monitor light-induced cyt *c* reduction kinetics to dissect the altered step(s) of Q_o site electron-transfer reactions (Figure 5). It is known that the extent of cyt *c* that remains oxidized upon flash activation of chromatophore membranes containing a wild-type bc_1 complex is correlated to the extent of electron transfer from the Fe−S subunit to cyt c_1 (*26*−*28*). This extent depends on the presence of different Q_o site inhibitors, with its amount being smaller in the presence of myxothiazol, and larger in the presence of stigmatellin (*26*−*28*), which locks the extrinsic domain of the Fe−S subunit at the Q_o site (*10*) (Figure 5, panel A). Moreover, we have very recently demonstrated that electron-transfer kinetics from the initially reduced [2Fe2S] cluster of the Fe−S subunit to cyt c_1 heme also reflect the movement of the extrinsic domain of the Fe−S subunit from the Q_o site to cyt c_1 heme (see ref *15*, for a detailed discussion). Thus, a comparison of the extent of cyt *c* that remains oxidized upon flash activation of chromatophore membranes in selected mutants in the presence of myxothiazol or stigmatellin was undertaken. The trac-

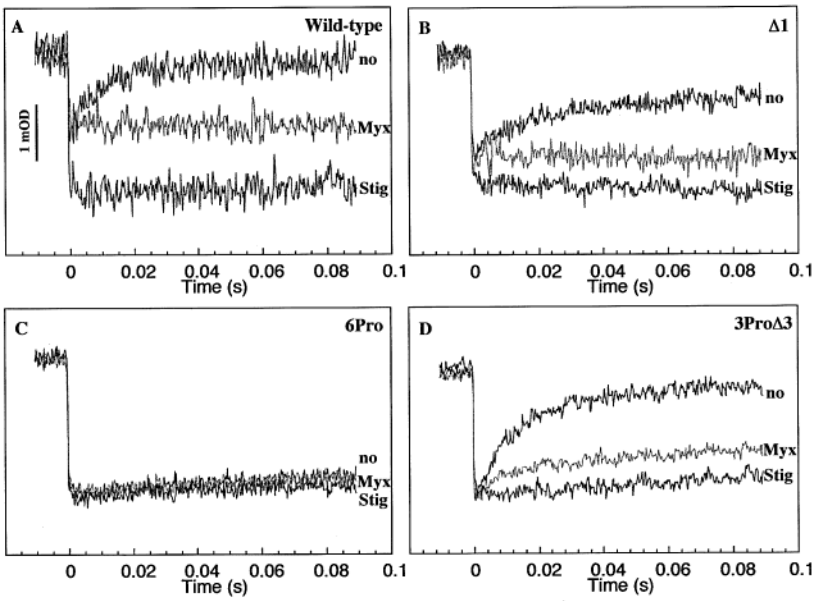

FIGURE 5: Cytochrome *c* rereduction kinetics in the presence of myxothiazol or stigmatellin in various Fe−S subunit hinge mutants. Cytochrome *c* rereduction kinetics triggered by flash-activation of the photochemical reaction center were recorded using chromatophore membranes as described in the Materials and Methods. In each case, the traces obtained with no inhibitor (no), or in the presence of myxothiazol (Myx) where no ubihydroquinone oxidation takes place at the Q_o site, or in the presence of stigmatellin (Stig) where no electron is transferred from the Fe−S subunit to cyt c_1 heme are shown. Panel A corresponds to the wild-type strain, panel B to the Δ1 mutant, panel C to the 6Pro mutant, and panel D to the Ps^+ revertant 3ProΔ3 of the 6Pro mutant.

es obtained in the presence of inhibitors with the Δ1 mutant were similar to those seen with a wild-type strain (Figure 5, panels A and B). However, traces obtained with the 6Pro mutant revealed that the amount of cyt *c* that stayed oxidized did not change in the presence of myxothiazol or stigmatellin and remained identical to that seen in the absence of inhibitor (Figure 5, panel C). The 6Pro mutant behaved in the absence of inhibitor, or in the presence of myxothiazol, as if it had already been exposed to stigmatellin, and hence unable to transfer electrons from the [2Fe2S] cluster to cyt c_1 in the time scale of the measurements (100 ms). Stigmatellin is known to lock the extrinsic domain of the Fe−S subunit, and by doing so stops electron transfer from the [2Fe2S] cluster to cyt c_1 heme (*10*, *15*). Therefore, these findings strongly suggested that in the 6Pro mutant the Fe−S subunit extrinsic domain was locked in a stigmatellin-like position on the cyt *b* subunit, even in the absence of this inhibitor (*10*).

That the extrinsic domain of the Fe−S subunit of the 6Pro mutant was locked in a stigmatellin-like position was further confirmed by using a conformation-sensitive protease assay (*20*). We have found that treatment of wild-type chromatophore membranes with the proteolytic enzyme thermolysin (or a proteolytic activity that is naturally present in *R. capsulatus*) releases an approximately 18 kDa truncated form of the Fe−S subunit, which lacks its first 46 first amino acid residues. This cleavage is sensitive to the conformation of the Fe−S subunit hinge region and is inhibited by stigmatellin (*20*). Upon testing for conformation-sensitive protease assay, the Fe−S subunit of the 6Pro mutant exhibited a similar cleavage pattern both in the presence and absence of stigmatellin, and both in response to thermolysin, or to the endogenous protease activity (not shown). Considering that this mutant responds properly to stigmatellin as indicated by EPR spectroscopy (Figure 3), the data further confirmed that its Fe−S subunit was locked in a position similar to that observed with a wild-type bc_1 complex in the presence of stigmatellin.

Ps^+ Revertants of the 6Pro and 6Gly Mutants of R. capsulatus. The unusual high frequency of reversion to Ps^+ phenotype of the 6Pro and 6Gly mutants was exploited to further investigate the structure and function of the hinge region of the Fe−S subunit. Ps^+ revertants were selected on MPYE enriched media, and three such isolates were retained in each case. Determination of the DNA sequence of the region encoding the Fe−S subunit hinge region in these revertants, named 3ProΔ3 or 3GlyΔ3, revealed that this region now encoded only three proline or three glycine residues, with deletion of the other three proline or glycine residues (Table 1). The 3ProΔ3 and 3GlyΔ3 revertants therefore contained shorter hinge regions, containing PPP and GGG residues substituting for the native VKAMAS sequence, respectively. Their studies indicated that while the 3GlyΔ3 mutant grew like a wild-type strain under Ps growth conditions, the 3ProΔ3 mutant exhibited a slower growth rate, and both mutants contained lower amounts of bc_1 complex activities in their chromatophore membranes (Table 2). Analysis of the 3ProΔ3 revertant using light-activated kinetic spectroscopy in the presence of myxothiazol or stigmatellin further revealed that in this mutant electron-transfer ability from the reduced [2Fe2S] cluster of the Fe−S subunit to cyt c_1 heme was restored (Figure 5, panel D). However, the rate of electron transfer was slower than that seen in a wild-type strain, in agreement with its poor Ps growth phenotype. Moreover, the slower rate of cyt *c* reduction observed in the presence of myxothiazol indicated that the extrinsic domain of its Fe−S subunit was not as mobile as that of a native bc_1 complex. Importantly, the overall data demonstrated that a hinge region three residues shorter than its natural length and containing three consecutive proline residues could support Q_o site function of the bc_1 complex and Ps growth of *R. capsulatus*.

DISCUSSION

In this study, a detailed investigation of the role played by the flexible hinge region of the Fe−S subunit (corresponding to amino acid residues 43−49 in *R. capsulatus*) in the function of the bc_1 complex was undertaken using various mutations modifying its sequence, length and flexibility. The results described here, in conjunction with the data available in other organisms (*13*, *14*, *16*, *17*), now better define some of the properties of the flexible region of the Fe−S subunit that serves as a hinge for the movement of its extrinsic domain.

Our data highlighted several important points on the structure and function of the hinge region of the Fe−S subunit of the bc_1 complex. First, various point mutations obtained at positions 43, 44, 45, 47, and 49 of the Fe−S subunit indicated that no specific amino acid side chain at any one of these sites was absolutely required for a functional bc_1 complex. This conclusion was further supported by the Ps^+ revertant +3AlaΔ3 of the Ps^- +3Ala mutant (discussed in ref *15*) which carries an insertion of three Ala residues at position 46 followed by a deletion of the following three residues (Table 1). Such a mutant is identical to a double substitution M47A plus S49A and illustrates that multiple positions between the amino acid residues 43−49 of the Fe−S subunit can be readily substituted by alanine residues without loss of function. Nonetheless, some of the positions in this region, such as D43 and V44 (*29*), may be more critical for Q_o site stability and function than others, as also seen with the A86L and A92R mutants in yeast (corresponding to A42L and A48R in *R. capsulatus* numbering, respectively) (*16*).

Second, the Ps^+ deletion mutants Δ1, Δ3, and Δ5 indicated that the hinge region can be shortened by at least five amino acid residues and still yield a functional bc_1 complex. Considering that the bc_1 complex is overexpressed in our mutants, it is not unexpected that even the Δ5 mutant which contains only about 0.2 Fe-S subunit/bc_1 complex (Figure 2) can still produce enough active enzymes in vivo to support a wild type-like Ps growth (Table 2). Further, the 3GlyΔ3 revertant, which is equivalent to the Δ3 mutant, with its VAS residues substituted with GGG (Table 1), also confirmed the relatively innocuous effect of deleting or substituting several amino acid residues within the hinge region. These findings sharply contrast the effects observed with the insertion mutations, which are absolutely deleterious to the function of the bc_1 complex by restraining severely the movement of the extrinsic domain of the Fe−S subunit (*15*).

Tian et al. (*13*) have constructed in *R. sphaeroides* a hinge mutant lacking three amino acid residues corresponding to the A42-D43-V44 in *R. capsulatus*. Unlike the *R. capsulatus* Δ3 mutant, this *R. sphaeroides* mutant contained in chromatophore membranes a properly assembled but poorly functional bc_1 complex. The EPR signature of its [2Fe2S] cluster was modified with no g_x signal, indicating that the position of the Fe−S subunit extrinsic domain within the Q_o pocket was changed. The differences seen between these apparently similar mutants may be due to the slightly different locations of the deletions in the corresponding hinge regions.

The effects of the deletions on the bc_1 complex activity were seen more readily when DBH_2-dependent steady-state turnover assays, which employ detergent-dispersed membranes, were used instead of light activated single turnover assays with intact chromatophores (Table 2). This may be due to a weaker association of the mutant Fe−S subunits with the bc_1 complex in the presence of dodecyl maltoside used in the assay. Another possibility is that in the shorter hinge mutants the Fe−S subunits may be more prone to proteolytic cleavage by the detergent activated endogenous proteolytic activity present in the chromatophore membranes of *R. capsulatus* (*20*, *30*). Such a cleavage would yield a truncated form of the Fe−S subunit that could not assemble to the bc_1 complex and hence lead to nonfunctional subcomplexes (*22*, *31*). Shortening of the hinge region of the Fe−S subunit may also induce additional constraints on its hydrophobic anchor domain, perhaps displacing it out of the membrane and rendering the mutant bc_1 complexes less stable. It is noteworthy that in the dimeric crystallographic structures of the bc_1 complex (*9*−*11*), the anchor domain of the Fe−S subunit interacts mainly with a cyt *b* subunit belonging to one monomer, while its extrinsic domain does so with the cyt *b* subunit of the other monomer. The purified bc_1 complex from *R. capsulatus* forms mainly a dimer (over 75%, unpublished results), but it is unknown whether both the monomeric and dimeric forms of the bacterial enzyme are functional. Thus, whether the hinge region of the Fe−S subunit is implicated in the stabilization of the dimeric form of the bc_1 complex remains to be seen.

The most interesting data were obtained with mutants that increased the rigidity or the flexibility of the hinge region of the Fe−S subunit of the bc_1 complex. Mutants which replaced six of the native amino acid residues by six proline or six glycine residues altered more severely the function, rather than the stability or assembly, of the bc_1 complex. The bc_1 complex of the 6Gly mutant was unable to sustain a vigorous Ps growth and that of the 6Pro mutant was completely inactive. Low single turnover, and no DBH_2 dependent multiple turnover, activities could be detected in these mutants, albeit the presence of properly assembled bc_1 complexes with intact Q_o sites, as reflected by EPR spectroscopy. Further, the increased E_m values of their [2Fe2S] clusters indicated that the extrinsic domain of their Fe−S subunit was located in a position close to that seen in the presence of stigmatellin. Unfortunately, the extremely high frequency of reversion of the 6Gly mutant, possibly triggered by its long stretches of GGC repeats (Table 1), was prohibitive to its extensive analysis. It is noteworthy to mention that the hinge region of the Fe−S subunits of b_6f complexes also contains six glycine residues (*5*). In the case of *C. reinhardtii* chloroplast Fe−S subunit, these glycine residues can be replaced by alanines without altering the function, of the b_6f complex (*17*). This observation suggests that the hinge region of chloroplast enzymes may be naturally more flexible than that of their bacterial or mitochondrial counterparts.

In the case of the 6Pro mutant, cyt *c* reduction kinetics obtained in the presence of myxothiazol or stigmatellin indicated that electron transfer between the [2Fe2S] cluster and heme c_1 was abolished. This lack of function could be mediated either by the inability of the Fe−S subunit to move away from its Q_o to its cyt c_1 positions or by its improper docking onto cyt c_1, as analyzed very recently with mutants containing alanine insertions in their hinge regions (*15*). The

higher E_m value of the [2Fe2S] cluster, and the protease mediated cleavage pattern of the Fe−S subunit strongly support the possibility that in the 6Pro mutant the [2Fe2S] cluster domain is locked in the Q_o pocket. During the thermolysin assays, we have noticed that higher amounts of intermediate size (between 24 and 18 kDa) of truncated forms of the Fe−S subunit were produced with the 6Pro mutant both in the presence or absence of stigmatellin. This suggested that the hinge region of the Fe−S subunit of this mutant was cleaved with thermolysin somewhat differently than that of the wild-type bc_1 complex. Interestingly, the ability of the 6Pro mutant to yield a Ps^+ revertant like 3ProΔ3, in which the sequence VKAMAS is substituted by PPP (Table 1), indicates that the rigidity conferred by the proline substitutions becomes tolerable if the hinge region is shortened.

Tian et al. (*13*) have shown that in *R. sphaeroides*, a three proline and two proline substitutions at positions corresponding to 42−44 and 46 and 48 in *R. capsulatus* numbering, yielded a non functional mutant with an unstable bc_1 complex, and a poorly functional mutant producing an enzyme with increased activation energy, respectively. The results obtained with the 3ProΔ3 mutant suggest that this higher activation energy could be attributed to the movement of the Fe−S subunit which would have become the rate-limiting step of the Q_o site reaction in the *R. sphaeroides* mutant. Our hinge mutants suggest that the lack of Q_o site catalysis is caused not only by the rigidity of the hinge region per se but also by the hindrance of the movement of the extrinsic domain of the Fe−S subunit due to its increased probability to bump onto the *ef* loop of cyt *b*. Hence shortening the hinge region, as in the 3ProΔ3 revertant, attenuates this physical hindrance and yields a Ps^+ mutant, whereas the *R. sphaeroides* 3Pro mutant of Tian et al., which contains a native length hinge produces a nonfunctional bc_1 complex and is Ps^- (*13*).

In summary, molecular genetic and biochemical-biophysical studies presented here using *R. capsulatus* mutants affecting the hinge region of the Fe−S subunit, and their revertants, revealed several important properties of this region. A shorter hinge region affects more strongly the assembly and stability of the Fe−S subunit than the activity of the bc_1 complex. Moreover, the amino acid sequence of the hinge region is less critical than its optimal length and flexibility in respect to Q_o site catalysis, and multiple combinations of amino acid compositions and lengths are readily functional, illustrating its structural flexibility. Future studies uncovering distant suppressors of the Fe−S subunit hinge mutants should allow a better definition of the different domains involved in controlling the movement of Fe−S subunit that orchestrates the bifurcated electron-transfer reactions at the Q_o site.

ACKNOWLEDGMENT

We would like to thank B. R. Gibney for assistance with the EPR machine.

REFERENCES

1. Knaff, D. B. (1993) *Photosynth. Res. 35*, 117−133.
2. Gennis, R. B., Barquera, B., Hacker, B., Van, D. S. R., Arnaud, S., Crofts, A. R., Davidson, E., Gray, K. A., and Daldal, F. (1993) *J. Bioenerg. Biomembr. 25*, 195−209.
3. Brandt, U., and Trumpower, B. (1994) *Crit. Rev. Biochem. Mol. Biol. 29*, 165−197.
4. Gray, K. A., and Daldal, F. (1995) in *Anoxygenic Photosynthetic Bacteria* (Blankenship, R. E., Madigan, M. T., and Bauer, C., Eds.) Kluwer Academic Publishers, Dordrecht, The Netherlands, pp 747−774.
5. Cramer, W., Soriano, G., Ponomarev, M., Huang, D., Zhang, H., Martinez, S., and Smith, J. (1996) *Annu. Rev. Plant Physiol. 47*, 477−508.
6. Mitchell, P. (1976) *J. Theor. Biol. 62*, 327−367.
7. Crofts, A. R., Meinhardt, S. W., Jones, K. R., and Snozzi, M. (1983) *Biochim. Biophys. Acta 723*, 202−218.
8. Ding, H., Robertson, D. E., Daldal, F., and Dutton, P. L. (1992) *Biochemistry 31*, 3144−3158.
9. Xia, D., Yu, C.-A., Kim, H., Xia, J. Z., Kachurin, A. M., Zhang, L., Yu, L., and Deisenhofer, J. (1997) *Science 277*, 60−66.
10. Zhang, Z., Huang, L., Shulmeister, V. M., Chi, Y.-I., Kim, K. K., Hung, L.-W., Crofts, A. R., Berry, E. A., and Kim, S.-H. (1998) *Nature 392*, 677−684.
11. Iwata, S., Lee, J. W., Okada, K., Lee, J. K., Iwata, M., Rasmussen, B., Link, T. A., Ramaswamy, S., and Jap, B. K. (1998) *Science 281*, 64−71.
12. Kim, H., Xia, D., Yu, C.-A., Xia, J.-Z., Kachurin, A. M., Zhang, L., Yu, L., and Deisenhofer, J. (1998) *Proc. Natl. Acad. Sci. U.S.A. 95*, 8026−8033.
13. Tian, H., Yu, L., Mather, M. W., and Yu, C.-A. (1998) *J. Biol. Chem. 273*, 27953−27959.
14. Tian, H., White, S., Yu, L., and Yu, C.-A. (1999) *J. Biol. Chem. 274*, 7146−7152.
15. Darrouzet, E., Valkova-Valchanova, M., Moser, C. C., Dutton, P. L., and Daldal, F. (2000) *Proc. Natl. Acad. Sci. U.S.A. 97*, 4567−4572.
16. Obungu, V. H., Wang, Y., Amyot, S. M., Gocke, C. B., and Beattie, D. S. (2000) *Biochim. Biophys. Acta 1457*, 36−44.
17. De Vitry, C., Finazzi, G., Baymann, F., and Kallas, T. (1999) *Plant Cell 11*, 2031−2044.
18. Atta-Asafo-Adjei, E., and Daldal, F. (1991) *Proc. Natl. Acad. Sci. U.S.A.* 88, 492−496.
19. Lowry, O., and Rosebrough, N. (1951) *J. Biol. Chem. 193*, 265−275.
20. Valkova-Valchanova, M., Darrouzet, E., Moomaw, C. R., Slaughter, C. A., and Daldal, F. (2000) *Biochemistry 39*, 15484−15492.
21. Darrouzet, E., Mandaci, S., Li, J., Qin, H., Knaff, D. B., and Daldal, F., *Biochemistry, 38*, 7908−7917.
22. Saribas, A. S., Valkova-Valchanova, M., Tokito, M. K., Zhang, Z., Berry, E. A., and Daldal, F. (1998) *Biochemistry 37*, 8105−8114.
23. Dutton, P. L. (1978) *Methods Enzymol. 54*, 411−435.
24. Gray, K., Dutton, P. L., and Daldal, F. (1994) *Biochemistry 33*, 723−733.
25. Liebl, U., Sled, V., Brasseur, G., Ohnishi, T., and Daldal, F. (1997) *Biochemistry 36*, 11675−11684.
26. Robertson, D., Davidson, E., Prince, R., van den Berg, W., Marrs, B., and Dutton, L. (1986) *J. Biol. Chem. 261*, 584−591.
27. Saribas, A. S., Ding, H., Dutton, P. L., and Daldal, F. (1995) *Biochemistry 34*, 16004−16012.
28. Crofts, A. R., Hong, S., Zhang, Z., and Berry, E. A. (1999) *Biochemistry 38*, 15827−15839.
29. Brasseur, G., Sled, V., Liebl, U., Ohnishi, T., and Daldal, F. (1997) *Biochemistry 36*, 11685−11696.
30. Darrouzet, E., Valkova-Valchanova, M., and Daldal, F. (1999) in *Photosynthesis: Mechanisms and Effects* (Garab, G., Ed.) Vol. 3, pp 312−316, Kluwer Academic Press, Dordrecht, The Netherlands.
31. Valkova-Valchanova, M. B., Saribas, A. S., Gibney, B. R., Dutton, P. L., and Daldal, F. (1998) *Biochemistry 37*, 16242−16251.

BI000750L